Differential Mechanisms for Calcium-Dependent Protein/Membrane Association as Evidenced from SPR-Binding Studies on Supported Biomimetic Membranes†

Claire Rossi,‡ Johanne Homand,‡ Cécile Bauche,§ Hayfa Hamdi,‡ Daniel Ladant,*,§ and Joël Chopineau*,‡

UMR 6022 CNRS Université de Technologie de Compiègne, BP 20529, 60205 Compiègne Cedex, France, and URA 2185 CNRS, Département de Biologie Structurale et Chimie, Institut Pasteur, 28 rue du Docteur Roux, 75724 Paris Cedex, France

Received July 28, 2003; Revised Manuscript Received November 3, 2003

ABSTRACT: In this work, two different types of supported biomimetic membranes were designed to study the membrane binding properties of two different proteins that both interact with cellular membranes in a calcium-dependent manner. The first one, neurocalcin, is a member of a subfamilly of EF-hand calcium-binding proteins that exhibit a calcium-myristoyl switch. The second protein is a bacterial toxin, the adenylate cyclase produced by *Bordetella pertussis*, the causative agent of whooping cough. The biomimetic membranes constructed in this study were either hybrid bilayer membranes or polymer-tethered membranes. Hemimembrane formation was obtained in two steps: a monolayer of 1-octadecanethiol or octadecyltrichlorosilane was self-assembled on top of the gold or glass surface, respectively, and then the egg-phosphatidyl choline (PC) vesicle fused on the hydrophobic alkyl layer. Polymer-tethered membranes on solid support were obtained using *N*-hydroxysuccinimide (NHS)-terminated-poly(ethyleneglycol) (PEG)-phospholipids as anchoring molecules. Egg-PC/1,2-distearoyl-*sn*-glycero-3-phospho-ethanolamine-poly(ethyleneglycol)-*N*-hydroxy-succinimide (DSPE-PEG-NHS) mixture liposomes were injected on the top of an amine grafted surface (cysteamine-coated gold or silanized glass); vesicles were linked to the surface and disrupted, leading to the formation of a bilayer. The biomimetic membrane constructions were followed by surface plasmon spectroscopy, while membrane fluidity and continuity were observed by fluorescence microscopy. Protein/membrane binding properties were determined by resonance surface plasmon measurements. The tethered bilayer, designed here, is very versatile as it can be adapted easily to different types of support. The results demonstrate the potentialities of such polymer-tethered artificial membranes for the study of proteins that insert into biological membranes such as toxins and/or integral membrane proteins.

Supported phospholipid layers as models for biomembranes have attracted attention during the past two decades (*1*−*11*). When supported on a solid substrate, they can be used as electrical or chemical biosensors, but they can also constitute mimetic models for biological membranes that can bind or incorporate proteins under nondenaturing conditions.

Hybrid bilayer membranes (HBMs)[1] are commonly used as biomimetic membrane models, and numerous examples of HBMs have been previously described and well characterized (*5*, *12*−*15*). Phospholipid vesicles can adsorb, rupture, and lipids self-assemble onto a substrate bearing an alkylthiol monolayer. Thus, a planar monolayer of phospholipids is formed with phospholipids having their hydrocarbon tails oriented toward the chains of the alkylthiols and their polar head oriented toward the buffer. Although these biomimetic surfaces are well-defined and robust structures, they are only poor equivalent of authentic biological membranes. Indeed, integral membrane proteins can hardly be inserted in such bilayers in a functional state, mainly because of the rigidity of the covalently attached alkyl underlayer.

More appropriate models of biomimetic phospholipid bilayers must fulfill the following requirements:

(i) They should be fluid structures with two layers of authentic phospholipids.

(ii) They should delimit two distinct aqueous compartments ("cis" and "trans") on both sides of the bilayer.

† This work was supported by Centre National de la Recherche Scientifique, the Pasteur Institute, and Grant No. QLK2-CT-1999-00556 from the 5th Framework Program of the European Union.

* Corresponding authors: Joël Chopineau, UMR 6022 CNRS, Université de Technologie de Compiègne, BP 20529, 60205 Compiègne cedex, France. Tel: 33 3 44 23 44 55. Fax: 33 3 44 20 39 10. E-mail: Joel.chopineau@utc.fr. Daniel Ladant, URA 2185 CNRS, Département de Biologie Structurale et Chimie, Institut Pasteur, 28 rue du Docteur Roux, 75724 Paris cedex, France. Tel: 33 1 45 68 84 00. Fax: 33 1 40 61 30 43. E-mail: ladant@pasteur.fr.

‡ UMR 6022 CNRS Université de Technologie de Compiègne.

§ URA 2185 CNRS, Département de Biologie Structurale et Chimie, Institut Pasteur.

[1] Abbreviations: HBM, hybrid bilayer membranes; TLB, tethered lipid bilayers; SPR, surface plasmon resonance; CyaA, adenylate cyclase toxin; proCyaA, nonacylated inactive adenylate cyclase protoxin; ADMS, aminopropyl-dimethylethoxysilane; OTS, 1-octadecyltrichlorosilane; egg-PC, L-α-phosphatidyl choline from egg yolk; DPPE-NBD, 1,2-dipalmitoyl-*sn*-glycero-3-phosphoethanolamine-*N*-7-nitro-2,1,3-benzoxadiazol-4-yl; DSPE-PEG$_{3400}$-NHS, 1,2-distearoyl-*sn*-glycero-3-phospho-ethanolamine-poly-(ethyleneglycol)-*N*-hydroxy-succinimide; HEPES, (*N*-{2-hydroxyethyl}piperazine-*N*′-{2-ethanesulfonic acid}); DTT, dithiothreitol; SDS−PAGE, sodium dodecyl sulfate−polyacrylamide gel electrophoresis; FRAP, fluorescence recovery after photobleaching; EGTA, ethylene glycol-bis(b-aminoethyl ether)-*N*,*N*,*N*′,*N*′-tetraacetic acid.

10.1021/bi035336a CCC: $25.00
Published on Web 12/06/2003

(iii) They should be defect-free to avoid preferential channels for electrons, ions, and/or small molecules.

(iv) Their preparation should be easy, reproducible, robust, and stable for long periods of time.

(v) This membrane-like structure should be assembled on different types of surfaces to allow various types of detection or analysis.

The simplest model developed in the pioneer work of the McConnell group (*1*, *2*) consisted of a single phospholipid bilayer that was deposited on glass over a thin water layer (10−25 Å). This original design has been improved in the recent years. To minimize the interactions between the bilayer and the hydrophilic solid support, the water layer has been replaced by an ionic layer consisting either of water compatible polymers (*16*−*18*) or of polyamines that electrostatically interact with the carboxylic groups of the alkylthio acids adsorbed onto gold (*19*, *20*).

The polymer cushion has a double role: it serves as a lubricant between the solid support and the fluid phospholipid bilayers, and it decreases the nonspecific binding of macromolecules to the surface. The most recent implementation of this type of biomimetic membrane consists of the covalent tethering of the polymer molecules to the surface support. In this case, the assembly/construction of stable tethered lipid bilayers (TLB) was achieved through a specific in situ polymerization procedure (*21*) or by using specific anchoring molecules such as functionalized lipid polymers (*22*−*26*). The main drawback of these approaches is that different coupling molecules should be designed and synthesized specifically for each particular type of support (e.g., thiols for gold surfaces, silanes for quartz or mica surfaces, etc.).

Assembly of biomimetic membranes on a solid surface offers attractive possibilities to monitor and characterize interactions of biomolecules with such membrane-like structures by using various sensitive biochemical techniques such as surface plasmon resonance (SPR) spectroscopy (*16*, *27*−*29*), electrical impedance (*30*−*32*), quartz crystal microbalance, (*33*−*35*), fluorescence microscopy (*36*), or atomic force microscopy (*37*−*39*).

Membrane interactions of different molecules including proteins have been investigated using biomimetic membrane constructions supported on solid surfaces. For example, reconstitution of different pore-forming molecules in tethered membranes have been reported. Valinomycin and gramicidin added directly in the aqueous phase were shown to insert spontaneously into preformed tethered membranes, while their selectivity toward antibiotics was maintained (*23*, *40*). More recently, an anion channel from *Clavibacter* was inserted in an electrostatically attached solid supported membrane and the specific of the channel activity was demonstrated (*41*). Morevover, the integral membrane protein rhodopsin was reconstituted in biomimetic membranes in a functional state able to interact with its natural effector transducin (*4*). Nevetheless, the functional assembly of such membrane-imbedded proteins into supported bilayers is still not a trivial process: for example, the well characterized, pore-forming toxin α-hemolysin from *Staphylococcus* was only partially functional when reconstituted into supported bilayer membranes (*42*).

In this work, we describe a novel type of polymer-tethered phospholipid bilayer in which the biomimetic membrane is covalently linked to the surface. Such a covalent anchoring was achieved by means of an poly(ethylene glycol) (PEG) chain ($n = 77$) derivatized on one end with a phospholipid and on the opposite end with an activated *N*-hydroxysuccinimide (NHS) ester. The latter could react with an amine monolayer of cysteamine or aminopropyl-dimethylethoxysilane that could be deposited and self-assembled on top of a gold or glass surface, respectively. Phospholipids vesicles containing the NHS-PEG-phospholipid anchoring molecules were deposited onto the amine-covered surface and, as a result of osmotic stress, large areas of continuous phospholipids bilayer were formed (as evidenced from fluorescence recovery after photobleaching (FRAP) experiments). The PEG moieties provide a hydrophilic medium and serve as a spacer between the amine-grafted surface and the phospholipid bilayer. Because the amine-grafted surface can be assembled on various supports such as gold, glass, quartz, or alumina by coating with appropriate amino-thiols or amino-silanes, construction of covalently tethered phospholipid bilayers could be extended to many support materials.

To demonstrate the utility of this type of biomimetic structure, we have investigated the membrane binding properties of two different proteins that both interact with membrane in a calcium-dependent manner. The first one, neurocalcin, is a member of a subfamily of EF-hand calcium-binding proteins that exhibit a calcium-myristoyl switch. The second protein is a bacterial toxin, the adenylate cyclase (CyaA) produced by *Bordetella pertussis*, the causative agent of whooping cough, that is able to translocate across the plasma membrane of eukaryotic target cells in a calcium-dependent manner. Interaction properties of these two proteins with the polymer-tethered membranes were analyzed by surface plasmon resonnance (SPR) spectroscopy, and their binding to a more classical hemimembrane biomimetic structure (HBM) was compared. Myristoylated neurocalcin was shown to interact with both types of biomimetic membranes in a calcium-dependent manner, whereas CyaA could only bind to the polymer-tethered membrane. Our results indicate that the polymer-tethered membranes are therefore particularly appropriate to study membrane association properties of proteins that insert into the membrane bilayer and should be useful to reconstitute integral membrane proteins in a functional state.

EXPERIMENTAL SECTION

Materials. (a) Chemicals. 2-Mercaptoethylamine (cysteamine hydrochloride) (≥ 99%), 1-octadecanethiol (98%), aminopropyl-dimethylethoxysilane (ADMS, 99%), 1-octadecyltrichlorosilane (OTS), L-α-phosphatidyl choline from egg yolk (egg-PC) type XVI-E, and 1,2-dipalmitoyl-*sn*-glycero-3-phosphoethanolamine-*N*-NBD (7-nitro-2,1,3-benzoxadiazol-4-yl) (DPPE-NBD, used as fluorescent probe) were purchased from Sigma-Aldrich (St Quentin-Fallavier, France). 1,2-Distearoyl-*sn*-glycero-3-phosphoethanolamine-poly-(ethyleneglycol)-*N*-hydroxysuccinimide (DSPE-PEG_{3400}-NHS) was from Shearwater Polymers (Huntsville, AL, US). Detergents octyl-glucoside and Triton X-100 were from Sigma-Aldrich. All other chemicals used in this work were of analytical grade. All buffers prepared from Milli-Q water (resistivity higher than 18.2 MΩ cm) were filtered and thoroughly degassed. Glass microscope slides, chromium, and gold were from Sigma-Aldrich.

(b) Proteins Preparation. Myristoylated bovine neurocalcin δ was obtained as a recombinant protein from *Escherichia coli* as previously described (*43*). Proteins were stored in 20 mM, HEPES-Na buffer, pH 7.4 containing 150 mM NaCl, 1 mM dithiotreitol (DTT). Expression and purification of adenylate cyclase (CyaA) from *Bordetella pertussis* were performed as previously described (*44*). Protein purity was checked by sodium dodecyl sulfate−polyacrylamide gel electrophoresis (SDS−PAGE). The protein content in purified preparations was determined from their absorbance at 280 nm using a molar extinction coefficient of 20 mM^{-1} cm^{-1} for neurocalcin and of 137 mM^{-1} cm^{-1} for CyaA.

Methods. The glass material used in this work was carefully cleaned in a sulfochromic acid solution (5% potassium dichromate in sulfuric acid. *Caution: this solution reacts violently with organics and should be handle with extreme care*) and thoroughly rinsed with Milli-Q water. Glass microscope slides were then dried under a nitrogen stream until use.

(a) Vesicles Formation. Egg-PC vesicles were obtained from a dried film formed from a lipid chloroform solution (5 mg/mL), by removing the organic solvent under a nitrogen stream followed by 12 h drying under vacuum. The dried lipid film was suspended in 20 mM HEPES-Na, pH 8, 150 mM NaCl, to obtain the desired lipid concentration. After resuspension and vigorous vortexing of the sample, the lipid suspension was extruded 19 times through 50-nm calibrated polycarbonate membranes using a syringe-type extruder (Liposofast, Avestin Inc., Ottawa, Canada).

DSPE-PEG-NHS containing vesicles were prepared from a mixed dried film obtained from lipids containing the anchoring molecule in chloroform. After resuspension of the lipid film in 20 mM HEPES-Na, pH 8, 150 mM NaCl, and vigorous vortexing, the liposomes were formed according to the same procedure. For fluorescence microscopy measurements, the fluorescent probe (DPPE-NBD) was incorporated at 2% molar ratio into the lipid chloroform solution.

The hydrodynamic mean diameters of vesicles were determined by quasielastic light scattering (Zetasizer 1000/3000, Malvern Instruments, U.K.).

(b) Fluorescence Microscopy. A confocal scanning light microscope (LSM 410, Micro Systems Zeiss, Germany) was used for FRAP experiments. Fluorescence microscopy experiments were carried out using a 400 μL measurement cell which was obtained from the top half of a spectrophotometer open cuvette glued to the pretreated microscope glass slides.

For hybrid bilayer membrane formation, a monolayer of OTS was self-assembled on the surface to facilitate hydrophobic adsorption of vesicles. This coating was obtained by a 15-min alkylation of the cleaned glass slides in a freshly prepared solution of OTS (2% w/w) in anhydrous hexadecane. The coated glass slides were extensively rinsed with toluene and ethanol and finally dried under a nitrogen flow. After the open cuvette was glued, 300 μL of the vesicle suspension (egg-PC/DPPE-NBD) was added over the dried surface and hemimembrane formation was checked.

For the tethered membrane, the freshly cleaned glass slides were silanized by immersion into an ADMS solution (2%, v/v) in toluene for 8 h, and then they were thoroughly rinsed with toluene, ethanol, and water before being dried in an oven at 110 °C. The open cuvette was glued to the surface, the cell was washed with buffer, then 300 μL of a vesicle suspension (egg-PC/ $DSPE\text{-}PEG_{3400}$-NHS/ DPPE-NBD) was added over the surface, and after the cell was rinsed for 8 h with buffer, bilayer formation was observed.

In a typical experiment, the measurement cell was placed on the stage of an inverted Zeiss microscope (Axiovert 135) equipped with a 40× oil-immersion objective NA 1.3 and was illuminated with a argon laser (488 nm, 15 mW). All measurements were controlled by the LSM4 software from Zeiss. The NBD fluorescent probe (1−2 mol %) was excited by an argon ion laser at 488 nm (blue light) and the emitted corresponding image (512 × 512 pixels corresponding to an area of 320 × 320 μm^2) was collected at 525 nm (bright green light) during a 4 s scan at zoom 1. A smaller area (45 × 45 μm^2, 40× objective and zoom 8) was bleached using the scanning mode at full power laser during 4 s. The fluorescence recovery was recorded with the same objective at zoom 1, at low laser power and 4 s scan. The image sequences were recorded via the integrated LSM4 software; in a typical sequence 10 images each 4 s after bleaching, and then 10 each 8 s and 10 each 40 s were taken. Quantitative analysis of the gray levels of the bleached area was performed to evaluate the fluorescence recovery.

Mobile fraction, M, and fluorescence recovery, $f(t)$, were respectively defined by the following equations:

$$M = [F(\infty) - F(0)]/[F(i) - F(0)] \quad (1)$$

$$f(t) = [F(t) - F(0)]/[F(i) - F(0)] \quad (2)$$

in which fluorescence at different time intervals before bleaching, $F(i)$, at time t on the photobleached area, $F(t)$, and at infinite time on the photobleached area, $F(\infty)$. $F(0)$ was determined from an extrapolation at time $t = 0$ of the function $F(t)$ as a function of square root of time.

Experimental fluorescence recovery curves were fitted according to a theoretical equation of fluorescence recovery as function of time by using the following equation (*45*, *46*):

$$f(t) = \exp(-2\tau_D/t)[I_0(2\tau_D/t) - I_1(2\tau_D/t)] \quad (3)$$

where I_0 and I_1 are modified Bessel functions, $\tau_D = w^2/4D$ is the characteristic diffusion time, w is the radius of the bleached area at $t = 0$, and D is the lateral diffusion coefficient. This theoretical equation was established for the particular case of a circular photobleached area. As in our case, the photobleached area, A, was a square. Thus, the characteristic diffusion time was adjusted to $\tau_D = A/4\pi D$. Experimental conditions were chosen to satisfy the classical hypothesis related to diffusion processes: the presence of an infinite reservoir of diffusive species and bleaching times are negligible compared to average diffusion times.

(c) Surface Plasmon Resonance Measurements. The absorption and desorption experiments were performed using SPR. SPR spectroscopy is well-known as a powerful technique for measurements of thin films (*47*). The method is based on excitation of the surface plasmons by p-polarized light at the noble metal−dielectric interface. Surface plasmons are described as electromagnetic evanescent waves propagating along the surface with a typical penetration depth of 200 nm. In this work, the Kretschmann configuration was used to create an evanescent field on the gold surface. The

gold-coated glass slide was vertically assembled with a 0.8-mL PTFE sample cell, and a 90° LaSFN9 prism ($n = 1.85$) was mounted with the glass slides using terphenyl monobromonaphthalene (Cargille Laboratories Inc, NJ) as a matching fluid ($n = 1.656$). Monochromatic p-polarized light from an He−Ne laser beam ($\lambda = 633$ nm) was reflected from the backside of the gold-coated glass slide. The SPR curve is a function of the refraction indexes of the materials at the film surface. A minimum reflectance corresponds to the excitation of electron plasmons, and the minimum angle shifts if the refraction indexes of the layer at the surface are modified by a value of $\Delta n = n_{layer} - n_{buffer}$. The geometrical thickness (Δd) of the adsorbed material can be determined from the angle shift ($\Delta\theta$), and the refractive indexes of each layer must be known for calculations. We used previously described values of $n = 1.5$ for long chain alkyl-thiols on gold (*48*) for phospholipids layers (*22*, *49*) and proteins (*50*, *51*). Reflectivity was recorded as a function of incident angle, and optical thickness was determined according to Fresnel equations using the Winspall program (Max-Planck Institute for Polymer Research, Mainz, Germany). Kinetics were measured at a fixed angle of 1° below the minimum angle. To determine the amount of protein bound to the biomimetic membrane, the optical thickness were converted to protein surface concentration using 1 ng/mm^2 for an optical thickness of 10 Å (*47*, *52*). All measurements were performed at 25 °C.

(d) Preparation of Supported Membranes on Gold Surfaces. Gold-coated glass slides were obtained by thermal evaporation under vacuum (Evaporator Edwards model Auto 306, rate 0.001−0.01 nm/s, pressure $2-3 \times 10^{-6}$ mbar). A gold layer of 47 ± 1 nm was deposited onto a chromium adhesion layer of 2 ± 0.5 nm.

(e) Hybrid Bilayer Membrane. A monolayer of 1-octadecane thiol was self-assembled on top of the gold surface to facilitate liposome-mediated hydrophobic adsorption. This coating was obtained by adsorption of 1-octadecane thiol (1 mM in ethanol, water (4/1) solution) onto bare gold and characterized as previously described (*12*). Before vesicles fusion, the hydrophobic-coated surface was cleaned by injection of 40 mM octyl-β-D-glucoside. Hemimembrane formation was obtained by injection the egg-PC vesicle suspension (4 mL at a flow rate of about 3 mL min^{-1}) over the surface. The cell was first washed with NaOH (4 mM, 5 mL) which was shown to stabilize the bilayer (*29*, *53*, *54*), and finally the cell was flushed during 1 h with 20 mM HEPES-Na, pH 7.5, 150 mM NaCl, at a flow rate of 1 mL min^{-1}.

(f) Tethered Membrane. The freshly prepared gold substrates were immersed overnight in a 2-mercaptoethylamine degassed solution (5 mM in pure ethanol). The coated slides were thoroughly rinsed with ethanol and dried under a nitrogen stream. They were stored under nitrogen before being used. For bilayer formation, 4 mL of vesicle suspension of egg-PC/DSPE-PEG$_{3400}$-NHS (egg-PC final concentration of 1.3×10^{-3} M with variable DSPE-PEG$_{3400}$-NHS molar ratios) in 20 mM HEPES-Na, pH 8, 150 mM NaCl, were injected over the surface at a flow rate of 3 mL min^{-1}. A 1 h minimum reaction time was necessary for vesicles anchoring and disruption. The cell was rinsed with the same buffer (10 min at a flow rate of 1 mL min^{-1}), then with NaOH (4 mM, 4 mL, 5 min), and finally flushed during 1 h with 20 mM HEPES-Na, pH 7.4, 150 mM NaCl, at a flow rate of 1 mL min^{-1}.

(g) Protein Binding Assays. CyaA, nonacylated proCyaA, and myr-neurocalcin solutions were diluted from stock solutions into 20 mM HEPES-Na, pH 7.4, 150 mM NaCl, containing 1 mM DTT. Diluted proteins solutions (0.02−10 μM) were filtered and thoroughly degassed, and 4 mL was injected into the SPR cell containing the preformed biomimetic membrane. Kinetics of protein absorption was monitored by measuring the reflectivity at a fixed angle of 1° below the minimum angle. After 10−30 min, calcium was added into the SPR cell to a final concentration of 2−4 mM; after stabilization of the SPR signal (usually 40 min) the cell was rinsed for 10−30 min with buffer at a flow rate of 1 mL min^{-1}.

For control experiments without calcium, proteins were diluted in 20 mM HEPES-Na, pH 7.4, 150 mM NaCl, 3 mM $MgCl_2$ and 1 mM EGTA.

In some experiments, a sodium carbonate solution (5 mL, 100 mM, pH = 11) was added for 40 min, to remove nonspecifically bound proteins. In other experiments, the biomimetic membrane was solubilized at the end of analysis by injection of 0.15% Triton X-100 or 40 mM octylglucoside, to check the stability of the basal SPR signal. Temperature was maintained at 25 °C.

RESULTS AND DISCUSSION

Formation and Characterization of Biomimetic Lipid Membranes. Construction of the biomimetic structures studied in this work are illustrated in Figure 1. The hybrid bilayer membrane was obtained by deposition of a monolayer of octadecane thiol on top of the gold surface of the SPR cell; then, egg-PC vesicles were fused on this hydrophobic alkyl layer. To construct the polymer-tethered phospholipid bilayers, a monolayer of 1-aminoethane thiol was first deposited on the gold surface. Then, phospholipids vesicles containing the NHS-PEG-phospholipid anchoring molecules were injected and allowed to react with the amine-covered surface. After completion of covalent coupling, buffer was flushed over the surface to obtain a continuous phospholipid bilayer as a result of osmotic stress.

(a) Surface Plasmon Resonance Spectroscopy. Kinetics of vesicle adsorption onto gold-coated glass-slide were followed for both constructions by SPR spectroscopy. The experimental SPR setup illustrated in Figure 1A was obtained from Max-Planck Institute for Polymer Research, Mainz, Germany. Formation of the biomimetic structures was followed as a function of time, and organic layer thickness was determined from Fresnel equations using the Winspall program that fits the reflectivity curves.

(1) Hybrid Bilayer Membrane. A monolayer of 1-octadecane thiol was self-assembled on top of the gold surface to facilitate subsequent vesicle fusion via hydrophobic interactions (*12*, *29*, *53*). In previous experiments of 1-octadecane thiol adsorption onto gold surfaces, layer thicknesses of 29 ± 2.5 Å have been determined (*12*, *54*, *55*). In our experimental design, best SPR curve fits with the Winspall program were obtained for an 1-octadecane thiol inner monolayer thickness of 29 ± 2.5 Å and a refractive index of 1.5. After 1-octadecane thiol monolayer formation and careful drying, the coated substrate was mounted with a

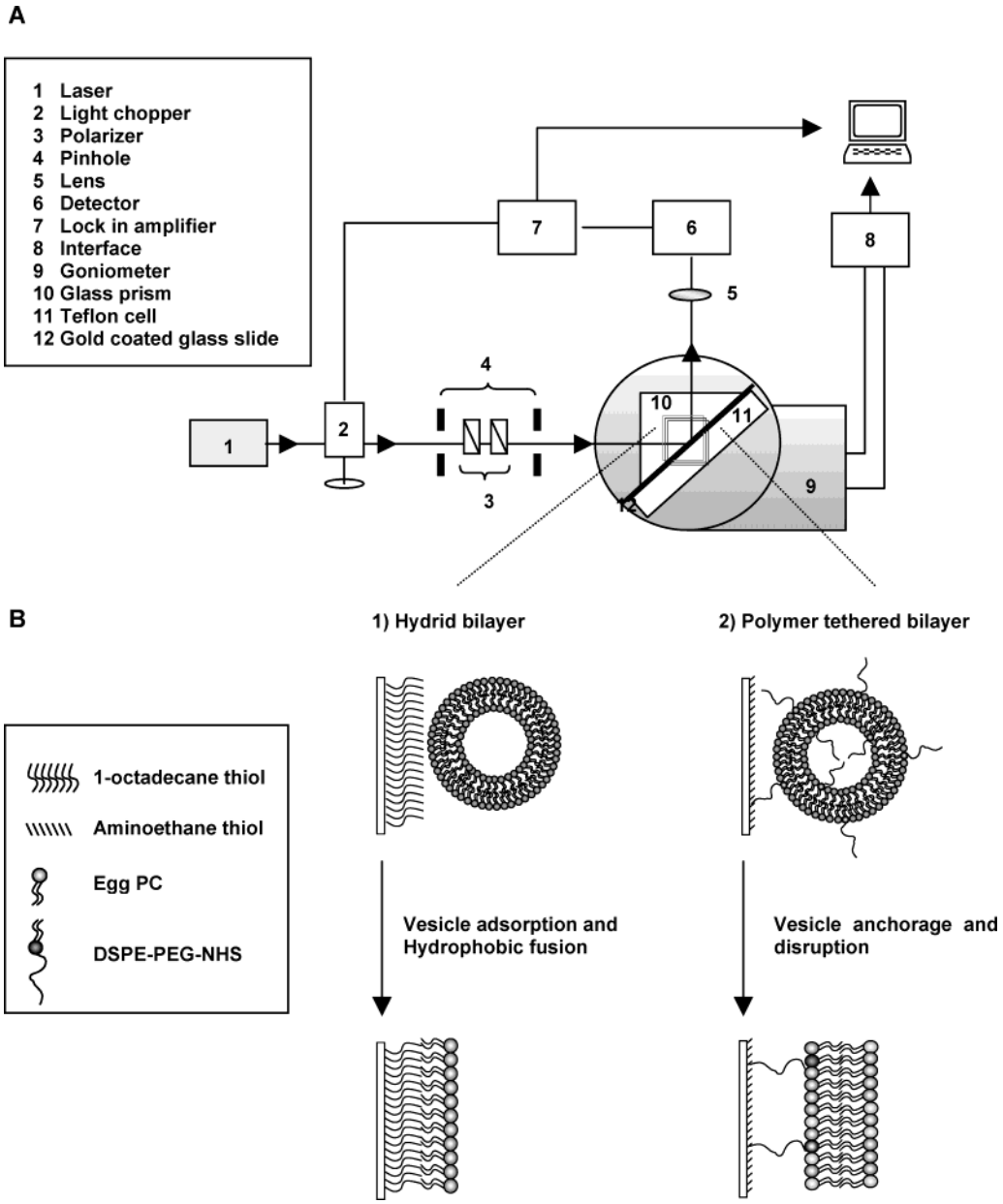

FIGURE 1: Biomimetic membrane formation followed by surface plasmon resonance (A) Scheme of the surface resonance plasmon set up from ref *12*. (B) Illustration of biomimetic membrane formation. (1) Hybrid bilayer membranes were obtained by self-assembling a monolayer of 1-octadecane thiol on gold on the top of which egg-PC vesicles were allowed to fuse and rupture. (2) Polymer-tethered bilayer formation starting from a self-assembled monolayer of cysteamine on gold-coated glass. The bilayer was formed from anchoring of mixed egg-PC/DSPE-PEG_{3400}-NHS liposomes followed by vesicle disruption.

Teflon cell and a spectrum was recorded. An egg-PC vesicle suspension (1 mg/mL) was injected onto the hydrophobic 1-octadecanethiol monolayer, and the fusion was recorded during 1 h. After rinsing the surface with buffer, Winspall calculations gave an average thickness of 22 ± 2.5 Å for the egg-PC layer, in agreement with the formation of a lipid monolayer (*12*, *29*). Altogether, the overall thickness of the biomimetic membrane was 50 ± 5 Å.

(2) Tethered Membrane. First, a cysteamine monolayer was deposited onto freshly prepared gold substrate and a reference SPR spectrum of this surface was recorded in HEPES-Na buffer. The thickness of the cysteamine monolayer adsorbed on gold was considered to be 5 Å according to ref *55*. Using this value, SPR data fitting gave a value of $n = 1.45$ for the cysteamine monolayer refractive index. These two parameters were used in all subsequent SPR calculations. Egg-PC vesicles containing various molar ratios of the anchoring molecule, DSPE-PEG-NHS (from 0 to 10 mol %), were injected over the surface. For molar ratios of anchoring molecules between 0.4 and 6 mol %, the vesicle adsorption kinetics were highly reproducible. Upon fitting the SPR reflectivity curves, the thickness of the adsorbed bilayer was estimated to be between 50 to 55 Å (Figure 2 A). When the anchoring molecule molar ratios were higher than 6 mol %, the kinetics of bilayer formation were poorly reproducible. The formation of vesicles, with such high density of anchoring molecules, is difficult to achieve due to the limited miscibility of DSPE within egg-PC bilayers.

Altogether, HBM and tethered bilayer membranes thickness calculated from SPR experiments were similar; a total of 48 or 51 Å (29 + 22 Å) was found for the HBM and the tethered bilayer was determined to be 50 to 55 Å. These

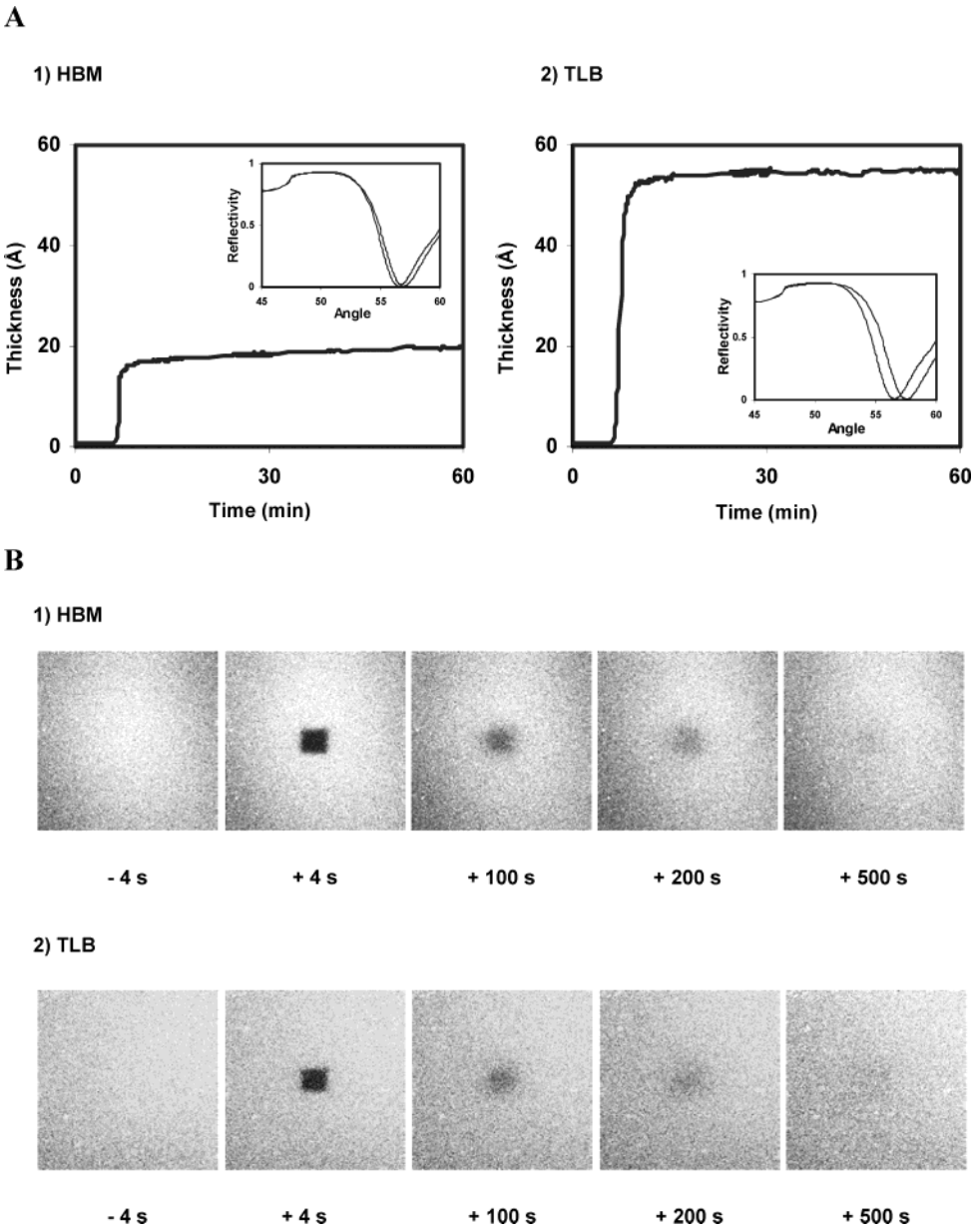

FIGURE 2: Characterization of the biomimetic membranes. (A) Surface plasmon resonance monitoring of the biomimetic membrane construction. (1) Egg-PC vesicle adsorption on the top of the self-assembled 1-octadecanethiol layer; (2) Egg-PC/DSPE-PEG$_{3400}$-NHS vesicle adsorption/anchorage onto the cysteamine-gold coated surface. Reflectivity as function of incident angle curves are shown in the corresponding insets. 1, curve at the lower angle is the SPR spectra of gold covered by 1-octadecanethiol and curve at the higher angle is the SPR spectra after lipid vesicle adsorption. 2, curve at the lower angle is the SPR spectra of gold covered by cysteamine and curve at the higher angle is the SPR spectra after lipid vesicle adsorption on amine covered gold substrate. (B) Fluorescence photobleaching images as a function of time in artificial egg-PC membranes. Images 320 × 320 μm, bleached area 45 × 45 μm. (1) Hydrid membrane was formed on glass using 1-octatrichlorosilane as a first layer according to the procedure described in Experimental Section. (2) Fluorescence photobleaching images of the fluorescent probe (NBD-DPPE, 2 mol %) in mixed egg-PC/DSPE-PEG$_{3400}$ bilayers; membrane was formed on amino-silanized glass surface.

two constructions share the same outer layer of egg-PC while the inner layer and the coupling to the substrate are different. The outer layer of polymer-tethered bilayer may contain up to half of the initial vesicular molar ratio of DSPE-PEG (i.e., 3 mol %), which is different from the hybrid bilayers (that are free of DSPE-PEG). Formation of hybrid bilayers incorporating DSPE-PEG is difficult to obtain because the presence of PEG chain impairs hydrophobic vesicular fusion.

(b) Fluorescence Microscopy Observations. Lateral diffusion coefficients and mobile fractions of the lipid probe (DPPE-NBD, 1−2 mol %) were determined from FRAP experiments carried out on a confocal microscope according to the recently described method (*56*). Briefly, after bleaching a small area (45 × 45 μm^2), the FRAP images (320 × 320 μm^2) were recorded at different time intervals to determine the fluorescence intensity recovery. To perform the FRAP experiments, the organic lipid layers had to be assembled on a glass support, transparent for the laser beam; therefore, the alkylthiols, cysteamine and 1-octadecane thiol, used above to coat the gold surface in the SPR mount, were replaced by silanes of corresponding length. After a first step of silanization of the glass surface, the procedures for bilayer constructions were identical to those used for the gold surfaces.

Results obtained for both types of biomimetic lipid membranes are shown in Figure 2B and Table 1 (reported

Table 1: FRAP Results on Glass Slides for Membrane Formation

first layer	vesicle composition	diffusion coefficient D ($cm^2\ s^{-1}$)	mobile fraction M (%)
OTS	egg-PC	$2.5 \times 10^{-8} \pm 0.5 \times 10^{-8}$	95 ± 5
ADMS	egg-PC/DSPE-PEG-NHS[a]	$2.4 \times 10^{-8} \pm 0.5 \times 10^{-8}$	95 ± 5
	egg-PC	$2 \times 10^{-8} \pm 0.5 \times 10^{-8}$	95 ± 5
ADMS	egg-PC	$1 \times 10^{-9} \pm 0.5 \times 10^{-9}$	40 ± 5

[a] DSPE-PEG-NHS/eggPC molar ratio: 2 mol %, experiments were carried at room temperature.

data from an average of six independent experiments). For the hybrid bilayer membrane, more than 95% of the fluorescent lipid probe were mobiles with a lateral diffusion coefficient of 2.5×10^{-8} $cm^2\ s^{-1}$ (Table 1, line 1). For the biomimetic tethered membrane (prepared with 2 mol % of anchoring molecules), we found that 95 to 98% of the fluorescent lipid probes were mobile with a lateral diffusion coefficient of 2.4×10^{-8} $cm^2\ s^{-1}$ (Table 1, line 2).

As a control, egg-PC vesicles were also deposited on cleaned glass, a hydrophilic substrate known to promote vesicle fusion (*1*, *2*). Our data ($D = 2 \times 10^{-8}$ $cm^2\ s^{-1}$, $M =$ 95%; Table 1, line 3) were indeed consistent with the formation of a continuous lipidic bilayer. In contrast, when pure egg-PC vesicles were deposited on amine-covered glass substrate, only a small fraction of the DPPE-NBD fluorescent lipid was mobile with a low lateral diffusion coefficient of 1×10^{-9} $cm^2\ s^{-1}$ (Table 1, line 4). The amine groups present a hydrophilic surface on which one would expect formation of a continuous bilayer. However, in our experimental conditions, we do not observe the formation of a continuous lipid bilayer either on a ADMS-coated glass surface (observed by FRAP measurements) or on cysteamine gold coated surfaces (monitored by SPR). The presence of an high density of protonated amino groups seemed to prevent a complete fusion which impaired the formation of a continuous lipid bilayer.

Altogether, our FRAP results indicate that both hybrid bilayers and tethered membranes could form a homogeneous and most likely continuous biomimetic membrane, lipid monolayer, or bilayer on the solid substrate, in good agreement with the data obtained in SPR experiments.

Interactions of Proteins with Biomimetic Membranes. To demonstrate that these biomimetic lipidic assemblies could be useful and relevant models for biological membranes, we attempted to characterize the interactions of known membrane-binding proteins with these artificial lipidic constructions.

For this study, we chose two different proteins that are known to bind to biological membranes in a calcium-dependent manner. The first one, neurocalcin, is a member of a subfamily of EF-hand calcium-binding proteins that exhibit a calcium-myristoyl switch (for a review, see ref *57*). These proteins are widely distributed in eukaryotes and may have very diverse functions, including activation of guanylate cyclase, regulation of G-protein coupled-receptor kinases, regulation of PI4 kinase, regulation of potassium channnels, and most likely many additional activities. The characteristic features of these proteins are (i) they are made of four EF-hand motifs, with only two or three being functional in calcium-binding; (ii) they are myristoylated on the N-terminal glycine residue; and (iii) most of them exhibit a calcium- and myristoyl-dependent binding to biological membranes, the so-called "calcium-myristoyl switch." Besides, for several members of this subfamily, the myristoyl group also seems to be important for their calcium-dependent association with target effector proteins (*57*).

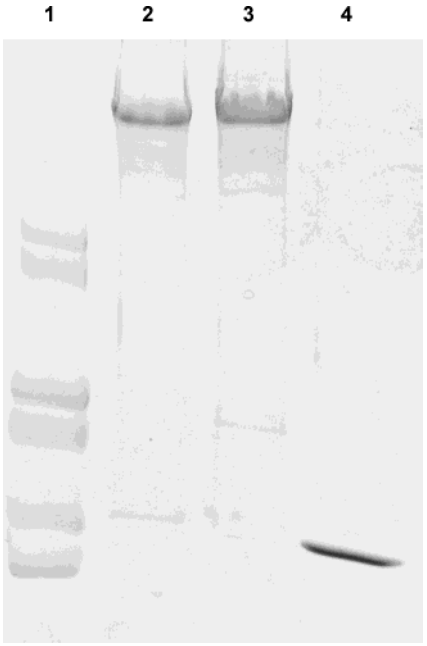

FIGURE 3: SDS−PAGE analysis of recombinant proteins. Samples of purified proteins were denatured in Laemmli sample buffer, run on a 5−15% SDS polyacrylamide gel, and stained with Coomassie blue. Lane 1: molecular mass markers corresponding, from top to bottom, to 94, 66, 43, 30, and 21 and 14 kDa; lane 2: 7 μg of purified CyaA; lane 3: 10 μg of purified proCyaA; lane 4: 10 μg of purified myr-neurocalcin.

The second protein is a bacterial toxin, the adenylate cyclase (CyaA) produced by *Bordetella pertussis*, the causative agent of whooping cough (*58*). This toxin is secreted by virulent bacteria and is able to translocate across the plasma membrane of eukaryotic target cells in a calcium-dependent manner. Upon reaching the cell cytosol, the adenylate cyclase catalytic domain (located in the first 400 residues of the 1706-amino acid long CyaA polypeptide) interacts with and is activated by the endogenous calmodulin to produce supraphysiologic levels of cyclic AMP. The CyaA toxin is also endowed with a hemolytic activity that is due to its ability to form cation-selective channels in lipid bilayers. Both internalization and hemolytic activities are calcium-dependent: CyaA binds about 40 calcium ions on a series of Gly and Asp-rich repeated motifs (called RTX, *R*epeat in *T*oxin) that have a rather low affinity for calcium (millimolar range). Interestingly, the CyaA toxin is also posttranslationally modified by specific acylation (palmitoyl or myristoyl groups) on two lysine residues, K860 and K983. This modification, which is carried out in the presence of the CyaC protein from *B. pertussis*, is essential to convert the inactive protoxin (proCyaA) into an active toxin able to interact with cell membrane and translocate into the target cell cytosol (for a review, see ref *58*).

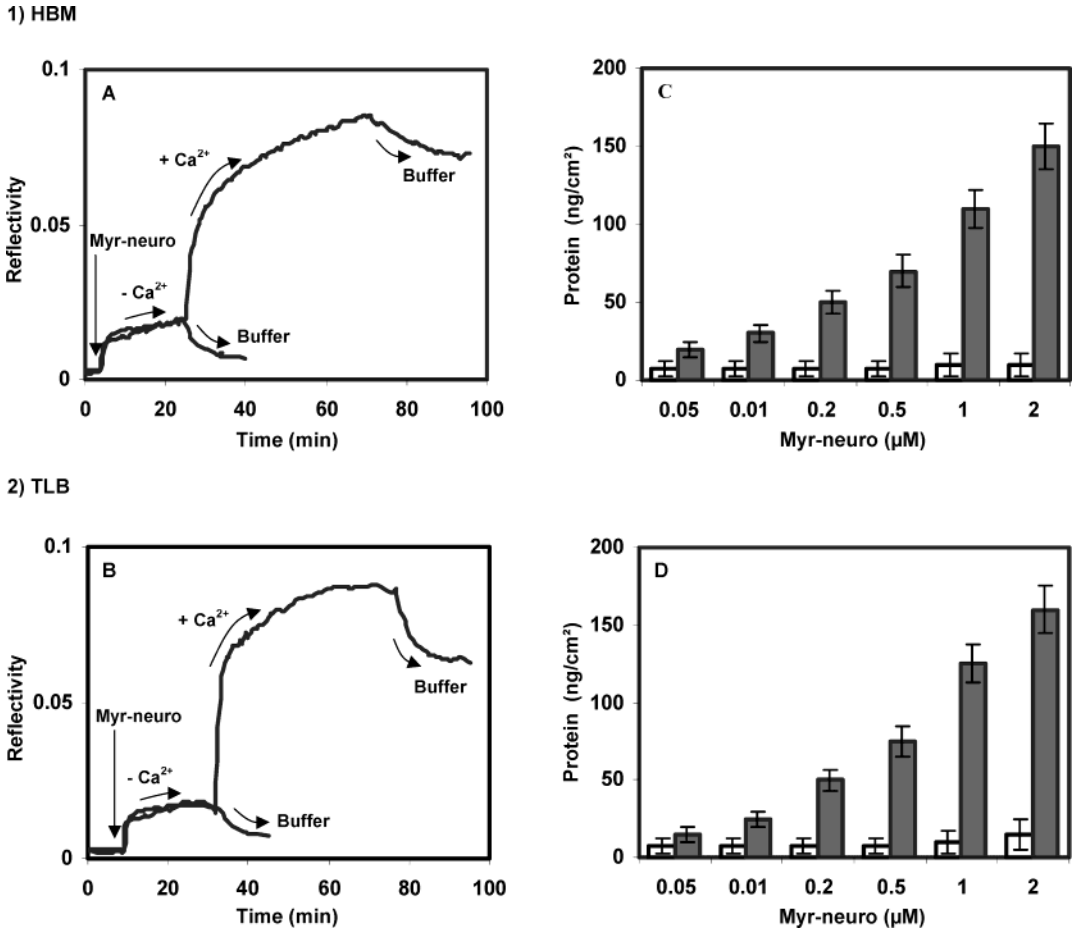

FIGURE 4: Biomimetic membrane binding properties of myr-neurocalcin on HBM (1) and TLB (2). (A, B) Overlay plots of SPR kinetic curves obtained for 2 μM myr-neurocalcin. Arrows indicate either presence or absence of calcium and buffer wash. (C, D) Surface protein bound quantities as a function of different myr-neurocalcin concentrations (0.05−2 μM), in the absence of calcium (white bars) and in the presence of calcium (gray bars). For calculation details see Experimental Section.

Although myr-neurocalcin and CyaA are both calcium- and acyl-dependent membrane binders, we anticipated that they should interact quite differently with the two types of artificial bilayers examined here. Indeed, calcium-bound myr-neurocalcin should behave as an extrinsic membrane protein, mainly attached to the membrane by means of its myristoyl group inserted in lipid bilayer and also through electrostatic interactions with the membrane surface. In contrast, calcium-bound CyaA should behave as an intrinsic membrane protein, with hydrophobic polypeptide segments putatively inserted within the lipid bilayer. Therefore, analysis of these two proteins should be useful to highlight the different properties of the two types of artificial membrane described here.

Both proteins were obtained as recombinant proteins expressed in *E. coli*, and they were purified to homogenity as previously described (*43*, *44*). An SDS−PAGE analysis of the purified proteins is shown in Figure 3.

Binding of proteins was investigated by performing SPR measurements according to the protocol described in Experimental Section. After formation of the hybrid bilayer or tethered membrane the proteins, diluted in 20 mM HEPES-Na, pH 7.4, 150 mM NaCl, were added either in the absence or in the presence of calcium. SPR spectra were recorded to quantify the amount of protein bound per membrane area which was determined from optical thickness using Winspall calculations (see details in Experimental Section).

Figure 4A,B shows a typical SPR record of myr-neurocalcin binding to either HBM or tethered membrane, respectively. Myr-neurocalcin bound efficiently to both types of artificial membranes in the presence of Ca^{2+}, while only a residual binding was observed in the absence of calcium. Interestingly, the myr-neurocalcin bound to both types of membrane could be almost completely removed upon washing by carbonate buffer (data not shown), which suggests that the protein was associated with the outer phospholipid layer without insertion. Similar binding assays were carried out on both types of membranes at different protein concentrations, as shown by Figure 4C,D. At the highest protein concentration tested, the maximal amount of myr-neuro per unit of surface determined from the SPR data, were similar on both types of membranes and correspond to about 150−160 ng/cm^2. These results are in good agreement with our previous studies performed in flow conditions on a hybrid bilayer membrane using the Biacore apparatus (*59*). In this previous work, the lipid layer was composed of brain lipids, and the maximum response (R_{max}) was about 1500 RU (resonance units) which corresponds to 150 ng of protein per square centimeter of membrane. In presence of calcium, the apparent affinity of myr-neurocalcin was found to be rather high with a K_D 0.35−0.40 μM (*59*).

The SPR analysis of CyaA binding to the two biomimetic surfaces are illustrated in Figure 5. In contrast to myr-neurocalcin, CyaA binding properties were drastically dif-

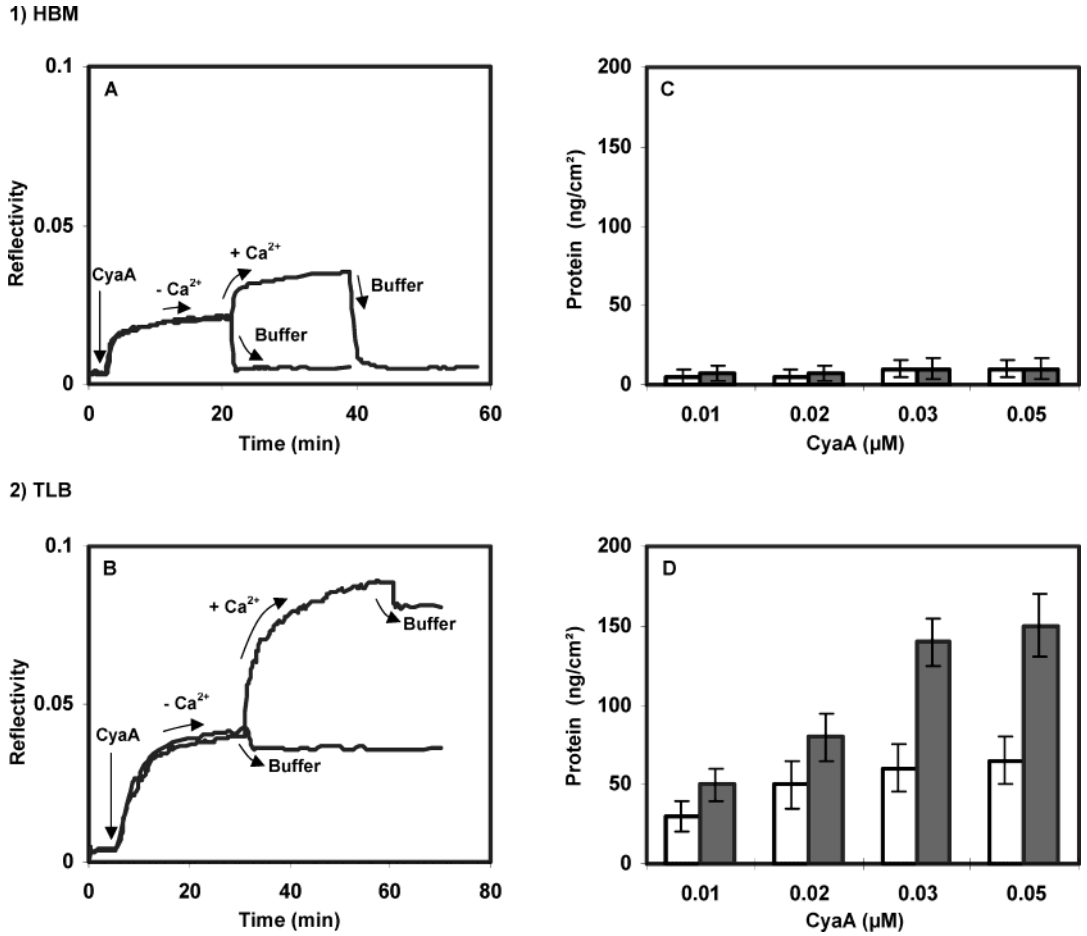

FIGURE 5: Biomimetic membrane binding properties of CyaA on HBM (1) and TLB (2). (A, B) Overlay plots of SPR kinetic curves obtained for 0.05 μM of CyaA. Arrows indicate either presence or absence of calcium and buffer wash. (C, D) Surface protein bound quantities as a function of different CyaA concentrations (0.01−0.05 μM), in the absence of calcium (white bars) and in the presence of calcium (gray bars). For calculation details see Experimental Section.

ferent on these two types of biomimetic surfaces. Indeed, CyaA bound efficiently to the polymer-tethered membrane in the presence of Ca^{2+} (Figure 5B), but it did not bind at all to the hybrid bilayer membrane (Figure 5A). CyaA interacts with biological membranes by inserting hydrophobic polypeptide segments into the lipid bilayer; therefore, hybrid bilayers offer only the outer layer in which CyaA was not able to insert. Furthermore, less than 10% of the CyaA bound protein could be removed from the polymer-tethered membrane upon extensive washing with carbonate buffer (data not shown). Altogether, these results suggest that CyaA associates with polymer-tethered membranes as a result of insertion of its polypeptide chain into the lipid bilayer and therefore it behaves as an integral membrane protein. These results are in full agreement with earlier characterizations of CyaA binding to eukaryotic target cells (*60*, *61*, *44*).

In absence of Ca^{2+}, the CyaA binding to the polymer-tethered membrane was drastically reduced (Figure 5B), and furthermore a large fraction (>60%) of the adsorbed protein could be removed upon washing by carbonate buffer (data not shown). This suggest that interactions of CyaA with this tethered membrane mimic association of the toxin with native cell membrane which was shown to be strictly Ca^{2+} dependent (*61*, *44*). In contrast, CyaA binding to liposomes suspensions was previously shown to be largely Ca^{2+} independent (DL, unpublished results). Therefore, the polymer-tethered membrane might represent a better substrate than

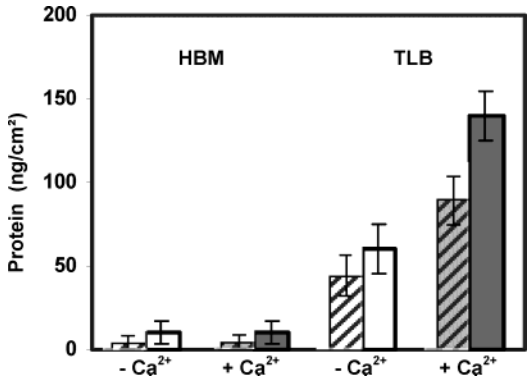

FIGURE 6: Membrane binding CyaA and proCyaA on HBM and TLB. Surface protein bound quantities obtained for 0.03 μM of CyaA (empty bars) and proCyaA (hatched bars) in the absence of calcium (white bars) and in the presence of calcium (gray bars).

liposomes to study CyaA interaction with eukaryotic cell membrane. Interestingly, Hyland et al. (*62*) reported that similarly, in the case of the alpha-hemolysin of *E. coli*, a related RTX toxin, Ca^{2+} binding did not influence the in vitro interaction with liposomes, although Ca^{2+} is required for toxin activity on eukaryotic target cells. Similar SPR binding assays were carried out on the polymer-tethered membrane at different CyaA toxin concentrations as shown in Figure 5D. The maximal amount of CyaA bound to the polymer-tethered membrane was found to be about 160 ng/cm^2 at the highest CyaA concentration tested of 50 nM.

We also examined the membrane binding properties of the nonacylated proCyaA protein on both types of artificial membranes. Figure 6 shows comparison of native CyaA and proCyaA properties, in the presence or in the absence of Ca^{2+}. As the acylated CyaA, proCyaA was unable to associate to the hybrid bilayer membrane. Yet, it did exhibit a significant binding to the tethered membrane which was partially calcium dependent.

CONCLUDING REMARKS

In this study, the calcium-dependent membrane binding properties of two different proteins were examined by SPR using two different types of supported biomimetic membranes. HBMs and polymer-tethered membranes were built on solid support, and mobility of a fluorescent probe followed by FRAP demonstrated fluidity and continuity of the membranes; their overall thickness were similar as determined from SPR measurements. The procedures allowing the construction of the biomimetic membrane relied on biocompatible (organic solvent free) and commercially available molecules. The main advantage of tethered phospholipid bilayer described here is that the same liposomal preparation could be easily assembled on various types of support. Indeed, the initial step, which consisted of the derivatization of a surface with amino groups by using self-assembled monolayers, could be easily performed on different types of support, such as glass or gold, as described here, and also alumina, mica, quartz, or other materials (*63*). These polymer-tethered membranes are therefore particularly appropriate to study membrane association properties of proteins that insert into the membrane bilayer and should be useful to reconstitute integral membrane proteins in a functional state. The advantage of such tethered phospholipid bilayers was further illustrated here by contrasting the mode of membrane association of two proteins, neurocalcin and CyaA, which are both calcium- and acyl-dependent membrane binders. Calcium-bound myr-neurocalcin behaves as an extrinsic membrane protein, mainly attached to the membrane by means of its myristoyl group inserted in lipid bilayer and also through electrostatic interactions with the membrane surface. In contrast, calcium-bound CyaA behaves as an intrinsic membrane protein, with hydrophobic polypeptide segments putatively inserted within the lipid bilayer. Therefore, the binding properties of these two proteins were able to distinguish between the different characteristics of the two types of artificial bilayers.

The hybrid bilayer membrane was able to bind the extrinsic binding protein myr-neurocalcin while almost no interaction was found in the case of CyaA, mainly due to the absence of a transmembrane compartment. Conversely, the polymer-tethered lipid membrane was found to be able to associate both types of proteins in a calcium-dependent manner. This latter should be therefore particularly appropriate to reconstitute authentic transmembrane proteins.

Moreover, because this type of covalently tethered bilayer membrane permits the defining of an aqueous compartment between the membrane and the supporting surface, it could be used to study transport of molecules across a biological membrane. This will be especially interesting in the case of the adenylate cyclase toxin, which exhibits the unique characteristics of invading eukaryotic target cells through a direct translocation across their plasma membrane. Although this process has been shown to be dependent upon the temperature (it occurs only above 15 °C), the membrane potential of the target cells (*64*), and the presence of calcium, the molecular mechanism of toxin internalization into target cells remains largely unknown. Our primary goal is now to set up a functional assay to detect the translocation of the catalytic domain across the supported bilayer. This should feasible as (i) a membrane potential (critical for the translocation process) can be established in such supported membranes, and (ii) the high catalytic activity of CyaA provides an exquisitely sensitive readout for quantification of the transfer of the catalytic domain of CyaA across the bilayer. This could open the way for a detailed biochemical and biophysical analysis of the CyaA translocation process across an artificial membrane. More generally, this type of covalently tethered bilayer should prove useful in the study of the translocation of polypeptide or protein across membranes.

ACKNOWLEDGMENT

The authors would like to thank C. Bourdillon for analysis of fluorescence experiments. We are grateful to W. Knoll for his unrestricted support.

REFERENCES

1. Brian, A. A., and McConnell, H. M. (1984) *Proc. Natl. Acad. Sci. U.S.A. 81*, 6159−6163.
2. Tamm, L. K., and McConnell, H. M. (1985) *Biophys. J. 47*, 105−113.
3. Sackmann, E. (1996) *Science 271*, 43−48.
4. Heyse, S., Ernst, O. P., Dienes, Z., Hofmann, K. P., and Vogel, H. (1998) *Biochemistry 37*, 507−522.
5. Plant, A. L. (1999) *Langmuir 15*, 5128−5135.
6. Salamon, Z., Brown, M. F., and Tollin, G. (1999) *Trends Biotechnol. 24*, 213−219.
7. Wong, J. Y., Majewski, J., Seitz, M., Park, C. K., Israelachvili, J. N., and Smith, G. S. (1999) *Biophys. J. 77*, 1445−57.
8. Wong, J. Y., Park, C. K., Seitz, M., and Israelachvili, J. (1999) *Biophys. J. 77*, 1458−1468.
9. Knoll, W., Frank, C. W., Heibel, C., Naumann, R., Offenhausser, A., Ruhe, J., Schmidt, E. K., Shen, W. W., and Sinner, A. (2000) *J. Biotechnol. 74*, 137−158.
10. Sackmann, E., and Tanaka, M. (2000) *Trends Biotechnol. 18*, 58−64.
11. Sackmann, E. (2000) *J. Biotechnol. 74*, 135−136.
12. Lingler, S., Rubinstein, I., Knoll, W., and Offenhäusser, A. (1997) *Langmuir 13*, 7085−7091.
13. Plant, A., Gueguetchkeri, M., and Yap, W. (1994) *Biophys. J. 67*, 1126−1133.
14. Plant, A., Brigham-Burke, M., Petrella, E. C., and O'Shannessy, D. J. (1995) *Anal. Biochem. 226*, 342−348.
15. Plant, A. (1993) *Langmuir 9*, 2764−2767.
16. Spinke, J., Yang, J., Wolf, H., Liley, M., Ringsdorf, H., and Knoll, W. (1992) *Biophys. J. 63*, 1667−1671.
17. Seitz, M., Wong, J. Y., Park, C. K., Alcantar, N. A., and Israelachvili, J. (1998) *Thin Solid Films 327*, 767−771.
18. Seitz, M., Ter-Ovanesyan, E., Hausch, M., Park, C. K., Zasadzinski, J. A., Zentel, R., and Israelachvili, J. (2000) *Langmuir 16*, 6067−6070.
19. Zhang, L., Booth, C. A., and Stroeve, P. (2000) *J. Colloid Interface Sci. 228*, 82−89.
20. Zhang, L., Longo, M. L., and Stroeve, P. (2000) *Langmuir 16*, 5093−5099.
21. Naumann, C. A., Prucker, O., Lehmann, T., Ruhe, J., Knoll, W., and Frank, C. W. (2002) *Biomacromolecules 3*, 27−35.
22. Lang, H., Duschl, C., and Vogel, H. (1994) *Langmuir 10*, 197−210.
23. Raguse, B., Braach-Maksvytis, V., Cornell, B. A., King, L. G., Osman, P. D. J., Pace, R. J., and Weiczorek, L. (1998) *Langmuir 14*, 648−659.

24. Théato, P., and Zentel, R. (2000) *Langmuir 16*, 1801−1805.
25. Wagner, M. L., and Tamm, L. K. (2000) *Biophys. J. 79*, 1400−1414.
26. Krysinski, P., Zebrowska, A., Michota, A., Bukowska, J., Becucci, L., and Moncelli, M. R. (2001) *Langmuir 17*, 3852−3857.
27. Duschl, C., and Knoll, W. (1988) *J. Phys. Chem. 88*, 4062−4069.
28. Cornell, B. A., Braach-Maksvytis, V. L., King, L. G., Osman, P. D., Raguse, B., Wieczorek, L., and Pace, R. J. (1997) *Nature 387*, 580−583.
29. Cooper, M. A., Try, A. C., Carroll, J., Ellar, D. J., and Williams, D. H. (1998) *Biochim. Biophys. Acta 1373*, 101−111.
30. Steinem, C., Janshoff, A., Ulrich, W.-P., Sieber, M., and Galla, H.-J. (1996) *Biochim. Biophys. Acta 1279*, 169−180.
31. Steinem, C., Janshoff, A., Galla, H.-J., and Sieber, M. (1997) *Bioelectrochem. Bioenerg. 42*, 213−220.
32. Gritsch, S., Nollert, P., Jahnig, P., and Sackmann, E. (1998) *Langmuir 14*, 3118−3125.
33. Keller, C. A., and Kasemo, B. (1998) *Biophys. J. 75*, 1397−1402.
34. Janshoff, A., Steinem, C., Sieber, M., El Baya, A., Schmidt, M. A., and Galla, H.-J. (1997) *Eur. Biophys. J. 26*, 261−270.
35. Pignataro, B., Steinem, C., Galla, H.-J., Fuchs, H., and Janshoff, A. (2000) *Biophys. J. 78*, 487−498.
36. Groves, J. T., Ulman, N., and Boxer, S. G. (1997) *Science 275*, 651−653.
37. Jass, J., Tjärnhage, T., and Puu, G. (2000) *Biophys. J. 79*, 3153−3163.
38. Dufrene, Y. F., and Lee, G. U. (2000) *Biochim. Biophys. Acta 1509*, 14−41.
39. Reviakine, I., and Brisson, A. (2000) *Langmuir 16*, 1806−1815.
40. Jenkins, A. T. A., Bushby, R. J., Boden, N., Evans, S. D., Knowles, P. F., Liu, Q., Miles, R. E., and Ogier, S. D. (1998) *Langmuir 14*, 4675−4678.
41. Michalke, A., Schurholz, T., Galla, H.-J., and Steinem, C. (2001) *Langmuir 17*, 2251−2257.
42. Glazier, S. A., Vanderah, D. J., Plant, A. L., Bayley, H., Valincius, G., and Kasianowicz, J. J. (2000) *Langmuir 16*, 10428−10435.
43. Ladant, D. (1995) *J. Biol. Chem. 270*, 3179−85.
44. Karimova, G., Fayolle, C., Gmira, S., Ullmann, A., Leclerc, C., and Ladant, D. (1998) *Proc. Natl. Acad. Sci. U.S.A. 95*, 12532−12537.
45. Axelrod, A., Kopel, D. E., Schlessinger, J., Elson, E., and Webb, W. W. (1976) *Biophys. J. 16*, 1055−1069.
46. Soumpasis, D. M. (1983) *Biophys. J. 41*, 95−97.
47. Knoll, W. (1998) *Annu. Rev. Phys. Chem. 49*, 569−638.
48. Spinke, J., Liley, M., Schmitt, F. J., Guder, H. J., Angermaier, L., and Knoll, W. (1993) *J. Chem. Phys. 99*, 7012−7019.
49. Reiter, R., Motschmann, H., and Knoll, W. (1993) *Langmuir 9*, 7012−7019.
50. Cuypers, P. A., Hermens, W. T., and Hemker, H. C. (1978) *Anal. Biochem. 84*, 56−57.
51. Spinke, J., Liley, M., Guder, H. J., Angermaier, L., and Knoll, W. (1993) *J. Chem. Phys.* 1821−1825.
52. Stenberg, E., Persson, B., Roos, H., and Urbaniczky, C. (1991) *J. Colloid Interface Sci. 143*, 513−526.
53. Pierrat, O., Lechat, N., Bourdillon, C., and Laval, J. M. (1997) *Langmuir 13*, 4112−4118.
54. Roy, M. O., Pugniere, M., Jullien, M., Chopineau, J., and Mani, J. C. (2001) *J. Mol. Recognit. 14*, 72−78.
55. Porter, M. D., Bright, T. B., Allara, D. L., and Chidsey, C. E. D. (1987) *J. Am. Chem. Soc. 109*, 3559−3568.
56. Berquand, A., Mazeran, P. E., Pantigny, J., Laval, J. M., and Bourdillon, C. (2003) *Langmuir 19*, 1700−1707.
57. Burgoyne, R. D., and Weiss, J. L. (2001) *Biochem J. 353*, 1−12.
58. Ladant, D., and Ullmann, A. (1999) *Trends Microbiol. 7*, 172−176.
59. Beven, L., Adenier, H., Kichenama, R., Homand, J., Redeker, V., Le Caer, J. P., Ladant, D., and Chopineau, J. (2001) *Biochemistry 40*, 8152−8160.
60. Rogel, A., and Hanski, E. (1992) *J. Biol. Chem. 267*, 22599−22605.
61. Rose, T., Sebo, P., Bellalou, J., and Ladant, D. (1995) *J. Biol. Chem. 270*, 26370−26376.
62. Hyland, C., Vuillard, L., Hughes, C., and Koronakis, V. (2001) *J. Bacteriol. 183*, 5364−5370.
63. Schreiber, F. (2000) *Prog. Surf. Sci. 65*, 151−157.
64. Otero, A. S., Yi, X. B., Gray, M. C., Szabo, G., and Hewlett, E. L. (1995) *J. Biol. Chem. 270*, 9695−9697.

BI035336A